Breather generation in fully nonlinear models of a stratified fluid

Kevin G. Lamb*
Department of Applied Mathematics, University of Waterloo, Waterloo, Canada N2L 3G1

Oxana Polukhina,† Tatiana Talipova, and Efim Pelinovsky
Department of Nonlinear Geophysical Processes, Institute of Applied Physics, Nizhny Novgorod, Russia

Wenting Xiao
Department of Mechanical Engineering, Massachusetts Institute of Technology, Cambridge, Massachusetts 02139, USA

Andrey Kurkin
Department of Applied Mathematics, State Technical University, Nizhny Novgorod, Russia
(Received 25 October 2006; published 19 April 2007)

Nonlinear wave motion is studied in a symmetric, continuously stratified, smoothed three-layer fluid in the framework of the fully nonlinear Euler equations under the Boussinesq approximation. The weakly nonlinear limit is discussed in which the governing equations can be reduced to the fully integrable modified Korteweg–de Vries equation. For some choices of the layer thicknesses the cubic nonlinear term is positive and the modified Korteweg–de Vries equation has soliton and breather solutions. Using such a stratification, the Euler equations are solved numerically using a sign-variable, initial disturbance. Breathers were generated for several forms of the initial disturbance. The breathers have moderate amplitude and to a good approximation can be described by the modified Korteweg–de Vries equation. As far as we know this is the first presentation of a breather in numerical simulations using the full nonlinear Euler equations for a stratified fluid.

DOI: 10.1103/PhysRevE.75.046306 PACS number(s): 47.20.Ky, 92.10.Dh, 05.45.Yv, 02.60.Cb

I. INTRODUCTION

Solitary internal waves are an important part of nonlinear wave motion in stratified fluids. In shallow water they can be described to leading-order by the Korteweg–de Vries (KdV) equation [1]. For certain stratifications—e.g., those with a buoyancy frequency profile that is nearly symmetric about middepth—the coefficient of quadratic nonlinearity can be anomalously weak or equal to zero, necessitating the inclusion of a cubic nonlinear term. This results in the extended Korteweg–de Vries (eKdV), or Gardner, equation which for rightward propagating waves has the form

$$\frac{\partial \eta}{\partial t} + c_0 \frac{\partial \eta}{\partial x} + \alpha \eta \frac{\partial \eta}{\partial x} + \alpha_1 \eta^2 \frac{\partial \eta}{\partial x} + \beta \frac{\partial^3 \eta}{\partial x^3} = 0, \qquad (1)$$

where $\eta(x,t)$ is the wave function describing the vertical displacement of an isopycnal, x is the horizontal coordinate, and t is time. All the coefficients are determined by integrals involving the unperturbed density profile $\bar{\rho}(z)$ and shear flow $U(z)$. Their expressions were first obtained for two-layer flow [2] and then for arbitrary (continuous or multilayer) fluid stratifications and background currents [3–5]. The Gardner equation is an integrable nonlinear evolution equation, and its multisoliton solutions can be found using modern techniques of nonlinear waves—e.g., the inverse scattering method, Hirota-Darboux transformation, etc. [6–9]. The existence of steady-state solitary wave solutions in the framework of the full nonlinear Euler equations can be proved using their reduction to the Dubreil–Jacotin-Long equation for the stream function $\psi(x,z)$ (e.g., [10,11]).

The nonlinear coefficients in Eq. (1) can have either sign, depending on the fluid stratification, while the dispersive coefficient β is always positive [5,12,13]. When the cubic nonlinear coefficient α_1 is negative, soliton solutions of a single polarity, with $\alpha\eta > 0$, exist with amplitudes between zero and a maximum, limiting value. If $\alpha_1 > 0$, solitons of either polarity exist. There is now no bound on the amplitude; however, those with $\alpha\eta < 0$ have a minimum amplitude. In addition there is a new type of solution, the breather, which, for example, can exist in the gap between the zero and minimum soliton amplitudes [14,15]. Breathers are periodically pulsating, or oscillating, isolated wave forms. Because they are not waves of permanent form, demonstrating the existence of fully nonlinear breathers is an extremely difficult task because there does not exist a reduction to more simplified equations like the Dubreil–Jacotin-Long equation.

The present paper has the goal of demonstrating the existence of breathers in the framework of the full nonlinear Euler equations. The Boussinesq approximation is used, as is appropriate for small density variations. Weakly nonlinear breather solutions are reviewed in Sec. II. In Sec. III the nonlinear numerical model is presented. Results of the fully nonlinear numerical simulations are presented in Sec. IV, and in Sec. V we present our conclusions.

II. WEAKLY NONLINEAR BREATHERS IN A STRATIFIED FLUID

One model stratification with a positive cubic nonlinear coefficient in Eq. (1) is a three-layer stratification with upper

*Electronic address: kglamb@uwaterloo.ca
†Also at Department of Applied Mathematics, State Technical University, Nizhny Novgorod, Russia.

and lower layers of equal thicknesses h and the same density jump $\Delta\rho$ across each interface. The total depth is denoted by H, and rigid boundaries at the top and bottom are used. For this symmetric stratification the quadratic nonlinear coefficient is zero and the Gardner equation reduces to the modified Korteweg–de Vries (mKdV) equation with coefficients [12,13]

$$c_0 = \sqrt{gh\Delta\rho/\rho_0},$$

$$\beta = \frac{c_0 h}{4}\left(H - \frac{4h}{3}\right), \quad \alpha_1 = -\frac{3c_0}{4h^2}\left(13 - \frac{9H}{2h}\right). \tag{2}$$

Here ρ_0 is the reference density used in making the Boussinesq approximation and g is the gravitational acceleration. The cubic nonlinear coefficient α_1 is positive only if $h/H < 9/26$—i.e., if the two interfaces are sufficiently far apart. Breather solutions of the mKdV equation are well known (e.g., [16]). In dimensional form, in a reference frame moving with the linear long-wave propagation speed c_0, they are

$$\eta(x,t) = -\frac{4qH}{\cosh\theta}\left[\frac{\cos\phi - (q/p)\sin\phi\tanh\theta}{1 + (q/p)^2\sin^2\phi\sinh^2\theta}\right], \tag{3}$$

where the"carrier" ϕ and "envelope" θ phases are

$$\phi = 2p\frac{x}{L} + 8p(p^2 - 3q^2)\frac{t}{T} + \varphi_0,$$

$$\theta = 2q\frac{x}{L} + 8q(3p^2 - q^2)\frac{t}{T} + \theta_0. \tag{4}$$

Here q and p are the spectral parameters in the associated Ablowitz-Kaup-Newell-Segur scheme [16] which characterize the breather amplitude (height) and the number of individual waves in the breather. ϕ_0 and θ_0 are initial phases, and the spatial and temporal scales of the breather,

$$L = \frac{1}{H}\sqrt{\frac{6\beta}{\alpha_1}}, \quad T = \frac{6}{\alpha_1 H^3}\sqrt{\frac{6\beta}{\alpha_1}}, \tag{5}$$

are functions of its amplitude and the coefficients of the mKdV equation. The "group" velocity of the breather in a reference frame moving with the linear long-wave speed c_0 is

$$V_{gr} = \frac{2}{3}\alpha_1 H^2(q^2 - 3p^2). \tag{6}$$

For large values of the parameter p the breather consists of many individual waves and represents an envelope soliton with amplitude $4qH$ propagating to the left. For small values of p the breather consists of a pair of solitary like form pulses of opposite polarities which oscillate. Its maximal absolute value changes in time with absolute maximum equal to $4qH$. It propagates to the left if $|q| < \sqrt{3}|p|$ and to the right if
$|q| < \sqrt{3}|p|$. In the limiting case $p \to 0$, the speed of the breather tends to the speed of a soliton with amplitude about $2qH$.

As mentioned above, the mKdV equation is an integrable equation and the Cauchy problem can be solved using the method of inverse scattering [16,17]. One of the analytical solutions of the associated spectral problem for the sign-variable rectangular-box initial conditions was obtained in Clarke *et al.* [18] where it was compared with direct numerical simulation of the mKdV equation.

III. NONLINEAR NUMERICAL MODEL

To study fully nonlinear breathers a numerical model based on the full nonlinear Euler equations under the Boussinesq approximation is used [3]. The idealized model equations are

$$\rho_0(\vec{U}_t + \vec{U}\cdot\vec{\nabla}\vec{U}) = -\vec{\nabla}P - \rho g\vec{k},$$

$$\rho_t + \vec{U}\cdot\vec{\nabla}\rho = 0,$$

$$\vec{\nabla}\cdot\vec{U} = 0. \tag{7}$$

These equations are solved in the vertical plane, so all physical fields are functions of x, z, and t. Here ρ_0 is the reference density, $\vec{U}=(u,w)$ is the velocity vector where u is the horizontal velocity in the x direction and w is the vertical velocity in the z direction, $\vec{\nabla}=(\frac{\partial}{\partial x},\frac{\partial}{\partial z})$ is the gradient operator, and P and ρ are the fluid pressure and density, respectively. The unperturbed density profile is a smoothed three-layer stratification of the form

$$\frac{\bar{\rho}(z)}{\rho_0} = 1 - \Delta\rho\tanh\frac{z-h_1}{d} - \Delta\rho\tanh\frac{z-h_2}{d}, \tag{8}$$

where the nondimensional density jump across each pycnocline is $\Delta\rho=0.005$. The other variables are nondimensionalized using the water depth H as the length scale and the buoyancy period $\tau=2\pi/N_b$ as the time scale where $N_b = \sqrt{4\Delta\rho g/H}$ is the bulk buoyancy frequency. The thickness of each transition layer is $d=0.04$. h_1 and h_2 are chosen to give upper and lower layer thicknesses of 0.3 and an intermediate layer thickness of 0.4. This gives a symmetric stratification which is a continuous approximation of a three-layer fluid with $h/H=0.3$, slightly less than 9/26. The bottom boundary is at $z=-1$ with z increasing upward. A vertical resolution of $dz=0.005$ and a horizontal resolution of $dx=0.05$ were used.

The initial condition has the form

$$\rho(x,z) = \bar{\rho}(y), \tag{9}$$

where the vertical Lagrangian variable y, which is the far stream height of an isopycnal, is given implicitly by

$$z = y + \zeta(x)\phi(y). \tag{10}$$

Here $\zeta(x)$ describes the initial horizontal structure and $\phi(y)$ is the mode-1 eigenfunction, obtained by solving the eigenvalue problem

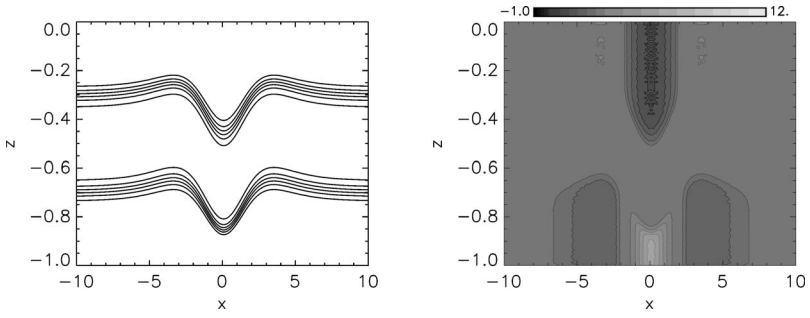

FIG. 1. Initial state for the numerical simulation in the reference frame in which fluid at infinity is at rest. Left panel: density contours. Right panel: horizontal velocity field.

$$\phi'' + \frac{N^2(y)}{c_0^2}\phi = 0, \tag{11}$$

with boundary conditions $\phi(-1)=\phi(0)=0$. The buoyancy frequency is given by $N^2(y)=-(g/\rho_0)d\bar{\rho}(y)/dy$. The eigenvalue c_0 is the mode-1 linear long-wave propagation speed which, in the three-layer limit, is given in Eqs. (2). The horizontal structure is chosen to be either a weakly nonlinear breather, with ζ given by Eq. (3), or in the form

$$\zeta(x) = a\left[2\mathrm{sech}^2\left(\frac{x}{L}\right) - 3\mathrm{sech}^4\left(\frac{x}{L}\right)\right]. \tag{12}$$

The velocity field is initialized in terms of the vertical displacement function $v(x,z)$ defined such that the rest height of the isopycnal passing through (x,z) is $y=z-v(x,z)$, implicitly given by Eq. (10). For an exact fully nonlinear internal solitary wave, the stream function in a reference frame moving with the wave is precisely $-cv(x,z)$ and the corresponding wave induced velocity field is $(-cv_z, cv_x)$ where c is the propagation speed of the solitary wave [19]. Thus, we choose to initialize the velocity field with $(-c_0 v_z, c_0 v_x)$ in our simulations. The simulation is done in a reference frame moving with speed c_0 to the left; thus, in initializing the velocity field we take $c_0<0$ for a leftward-propagating wave. The resulting initial state is not an exact solution of the governing equations; however, the initial density field satisfies all the conditions for breather solutions in the framework of the mKdV equation: it has zero mass and has a middle layer whose thickness is independent of x. Even when ζ is given by Eq. (3), the initial velocity field does not correspond to that of a weakly nonlinear breather, although it does satisfy the condition of having zero horizontal velocity perturbation in the middle layer.

IV. FULLY NONLINEAR BREATHER IN THE STRATIFIED EULER EQUATIONS

The first case we consider is a simulation initialized using Eq. (12) with $(a,L)=(0.16,3)$. The initial disturbance, shown in Fig. 1, is large. Consequently, the process of breather generation cannot be described in the framework of asymptotic theory. The fully nonlinear breather that emerges from this initial state is illustrated in Fig. 2 where the isopycnal displacements are shown at various times. After 106 bulk buoyancy periods the breather can be seen leading a mode-1 dispersive wave train, both of which are propagating leftward with respect to the fluid. At later times the breather emerges more clearly from the dispersive wave train. Its group velocity V_{gr} is less than c_0 in magnitude, so it is advected by the rightward background flow and never separates from the dispersive wave train. A Hovmüller plot of the surface velocity $u(x,0,t)$ is shown in Fig. 3 clearly illustrating the pulsating nature of the breather. The period of the oscillations and the propagation speed of the breather (in this reference frame) increase slightly at about $t=400$ and thereafter remain fairly constant. Nine full oscillations from the initial state can be seen illustrating the stability of the breather.

The nondimensional coefficients of the mKdV equation are $c_0=2.36$, $\beta=1121$, and $\alpha_1=29.5$. The amplitude of the breather after $t=400$, as defined by the maximum vertical displacement of the center of the upper pycnocline, varies between about 0.103 and 0.108. This gives a formal estimation of the nonlinear parameter $\alpha_1\eta^2/c_0$, which characterizes the nonlinear correction to the linear speed of propagation, of about 0.14 which is small but finite, suggesting that weakly nonlinear theory may be applicable and that the mKdV equation can be used to describe the propagation of the observed wave packets. Thus, the solution of the modified Korteweg–de Vries equation is used for comparison with results of the numerical simulation of the Euler equations.

Figure 4 compares the simulated and theoretical breathers at several times. To compare the fully nonlinear simulation

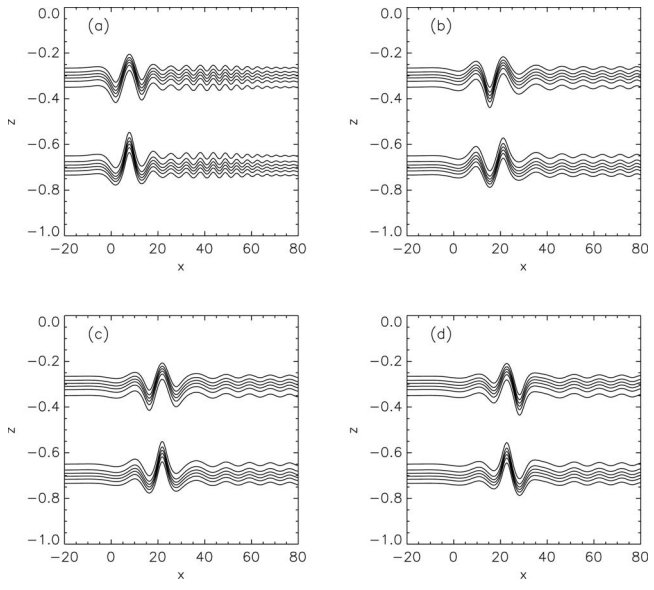

FIG. 2. Density contours showing the evolving wave field. (a) $t=106$. (b) $t=317$. (c) $t=388$. (d) $t=458$.

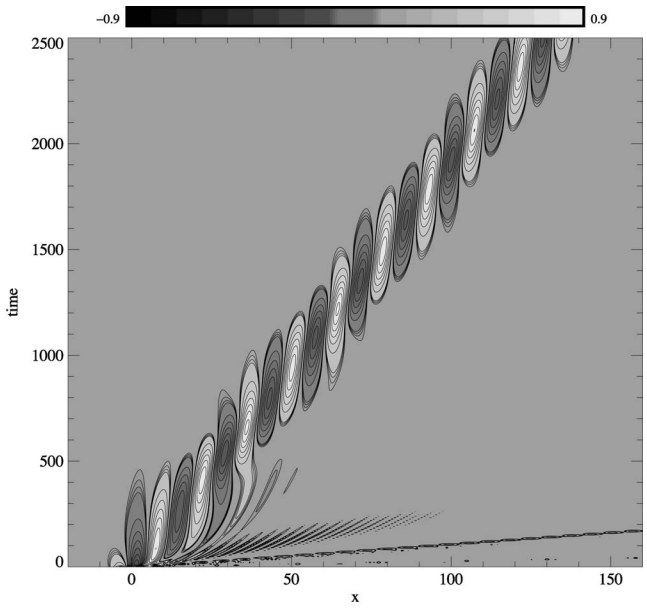

FIG. 3. Hovmüller plot of horizontal velocity perturbation at the surface. Contoured values are for magnitudes 0.1–0.9 in steps of 0.1 and between 0.07 and 0.1 in steps of 0.01.

with weakly nonlinear theory the breather parameters p and q must first be estimated. The value of $q=-0.026$ was determined from the maximum amplitude of the simulated breather at a time when the breather was horizontally symmetric with downward displacement at its center [Fig. 4(a)]. The value $p=0.0285$ was then chosen so that the oscillation periods of the fully nonlinear and weakly nonlinear breathers were the same. Panels (a)–(e) compare the initial breathers and their evolution every quarter of an oscillation period $\tau_{osc}\approx 282$ over one oscillation. Panel (f) compares the two after two oscillation periods. The number of oscillations in the breather, the width of the breather, and the amplitude of the two maxima to either side of the breather center are captured quite well by the values of p and q used, indicating that the mKdV equation provides a reasonably accurate description of the waves. The theoretical breather travels with velocity of $-(c_0-0.035)$ relative to the fluid [see Eq. (6)] while the fully nonlinear breather travels with a slower velocity of about $-(c_0-0.052)$. This propagation speed can be estimated from both Figs. 3 and 4. The difference in propagation speeds suggests that higher-order effects are of some importance. The other significant difference is that while the theoretical breather is vertically symmetric, in the sense that after half an oscillation period η is reversed in sign, this is not the case for the simulated breather. The simulated breather has a maximum downward displacement of about 0.1, and half an oscillation period later it has a maximum upward displacement of only 0.065 [Fig. 4(c)]. The two depressions to either side of the central peak are also smaller in the simulated breather. This is another indication that higher-order nonlinear effects are important.

Breathers were also simulated by initializing the model with a density field appropriate for weakly nonlinear breathers using Eq. (3) instead of Eq. (12). After some adjustment the final breather was similar to the initial one. For example,

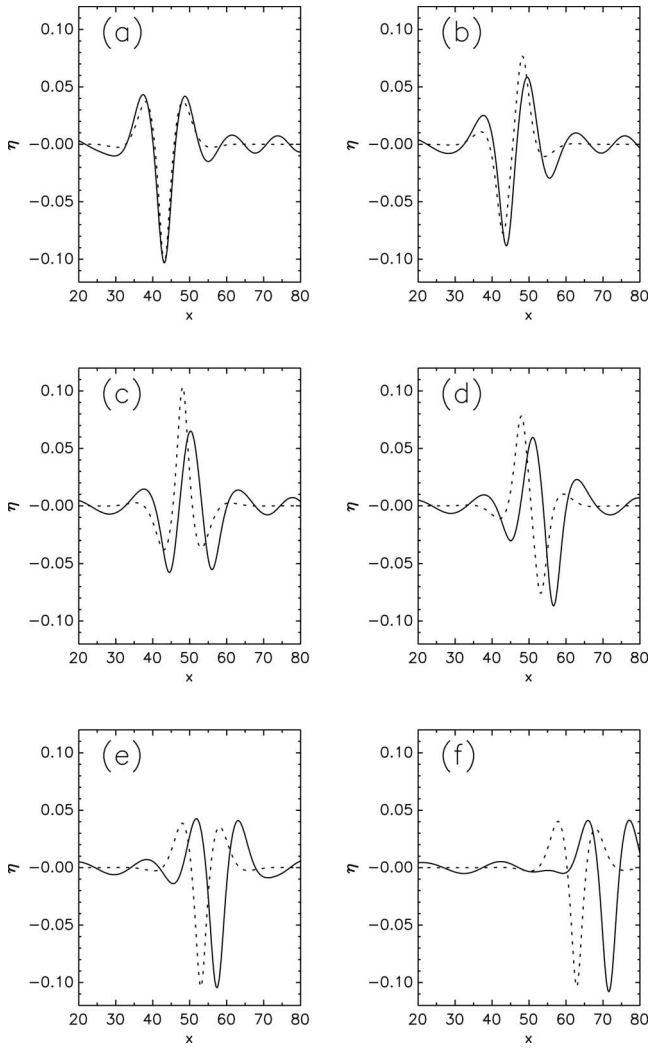

FIG. 4. Comparison of the vertical displacement of the upper pycnocline in the fully nonlinear breather (solid) and the weakly nonlinear breather (dots) at six different times. (a) $t=t_0=796.6$. (b) $t=867.1\approx t_0+0.25\tau_{osc}$. (c) $t=937.6\approx t_0+0.5\tau_{osc}$. (d) $t=1008.1\approx t_0+0.75\tau_{osc}$. (e) $t=1078.6\approx t_0+\tau_{osc}$. (f) $t=1353.5\approx t_0+2\tau_{osc}$. Here $\tau_{osc}=282$ is the breather oscillation period.

for an initial weakly nonlinear breather with $(p,q)=(0.0285,-0.026)$, the same values as the simulated breather shown in Figs. 2–4, the final breather had values of $(p,q)=(0.0272,-0.022)$. Breathers with multiple oscillations were also simulated. An example, initialized with $(p,q)=(0.1,-0.026)$, is shown in Fig. 5. The first panel shows the initial density field. The initial perturbation is not an exact breather, so an adjustment takes place. Some of the radiated waves move to the right relative to the fluid and hence propagate away with velocity greater than the long-wave propagation speed. These have already left the domain by $t=135.7$ [Fig. 5(b)]. The largest radiated waves, centered at $x=125$ at $t=135.7$, are mode-2 waves propagating to the left relative to the fluid but much more slowly than the mode-1 breather. The adjustment includes the generation of a small-amplitude dispersive wave train. Because the background flow is moving to the right with the linear long-wave speed, this wave train extends from its front at the initial location of the

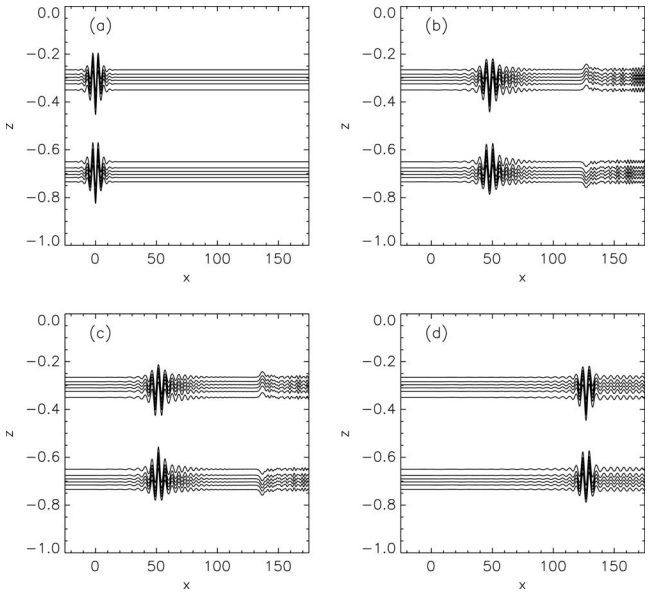

FIG. 5. Density contours showing the evolving wave field for a case initialized with a weakly nonlinear breather with parameters $(p,q)=(0.1,-0.026)$. (a) Initial weakly nonlinear breather at $t=0$. (b) $t=t_0=135.7$. (c) $t=146.3\approx t_0+0.5\tau_{osc}$. (d) $t=364.8\approx t_0+10\tau_{osc}$. Here $\tau_{osc}=22.9$ is the period of the simulated breather.

breather rightward to beyond the right boundary. A dispersive wave train of larger amplitude appears ahead and behind the breather. This wave train grows in length behind (to the right of) the breather [Figs. 5(b)–5(d)]. It is not known if this is an indication that exact, fully nonlinear breathers do not exist or if it is a consequence of a nonlinear interaction between the breather and the weak-dispersive wave train in which it is embedded.

Comparisons of this case with weakly nonlinear theory are made in Fig. 6. The parameters for the weakly nonlinear breather were fixed by fitting the simulated amplitude of the depression at the center of the breather at $t=135.7$, after the initial adjustment, and a period of oscillation of over ten oscillations. This fit yielded parameter values $(p,q)=(0.766,-0.024)$, indicating a decrease in magnitude of about 23% and 8% from the values used in the initialization. The comparison again shows an asymmetry in that after half an oscillation [Fig. 6(c)], the simulated elevation is significantly smaller than the initial depression. The size of the initial adjustment is partly a consequence of the fact that the initial velocity field is not taken from weakly nonlinear theory.

V. CONCLUSION

Numerical solutions of the full nonlinear Euler equations using an ideal, continuously stratified, smoothed three-layer fluid have demonstrated the existence of fully nonlinear breathers. There is some evidence to suggest they may slowly radiate energy in the form of a trailing small-amplitude dispersive wave train and hence they may not be exact breathers. The breathers forming in the nonlinear simulations are of moderate amplitude (approximately a third of

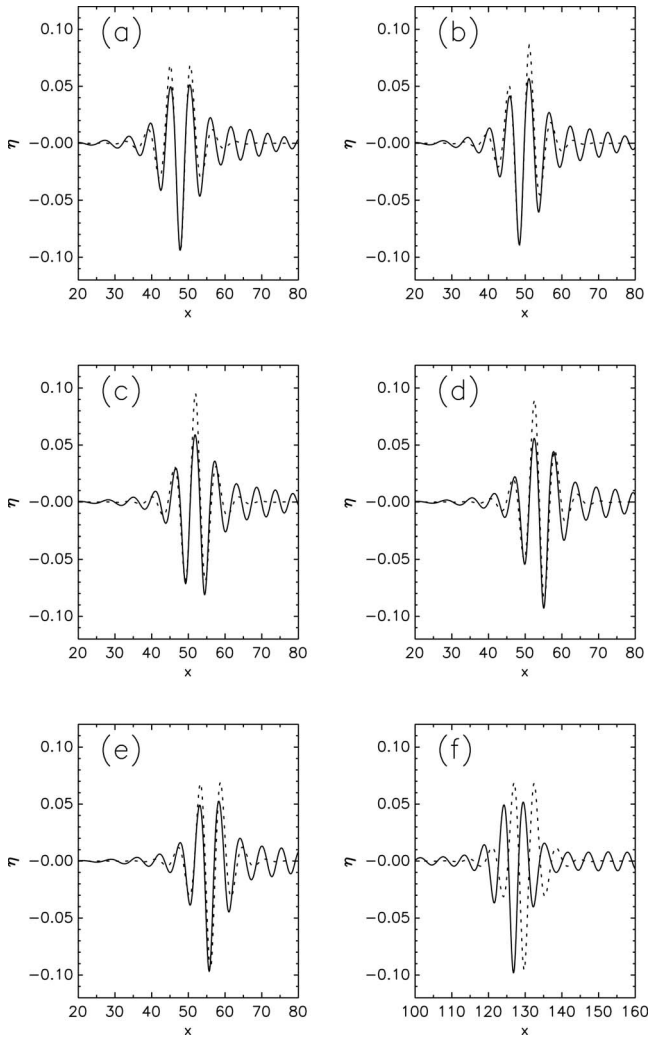

FIG. 6. Comparison of the vertical displacement of the upper pycnocline in the fully nonlinear breather (solid) and the weakly nonlinear breather (dots) at six different times for the case initialized with a weakly nonlinear breather. (a) $t=t_0=135.7$. (b) $t=141.0\approx t_0+0.23\tau_{osc}$. (c) $t=148.0\approx t_0+0.54\tau_{osc}$. (d) $t=153.3\approx t_0+0.77\tau_{osc}$. (e) $t=158.6\approx t_0+\tau_{osc}$. (f) $t=364.8\approx t_0+10\tau_{osc}$. Here $\tau_{osc}=22.9$ is the breather oscillation period.

the upper and lower layer thicknesses) and their properties are well described in the framework of the modified Korteweg–de Vries equation. Results from two simulations have been presented. The first, using the initial form (12), resulted in a breather with few oscillations (small p) and demonstrates that breathers can form from somewhat arbitrary conditions. Simulations using different initial amplitudes a and widths L were done, showing that breathers are only generated for a range of initial widths and amplitudes (results not shown). For example, for $(a,L)=(0.26,1.5)$ and $(a,L)=(0.08,3)$ only dispersive wave trains appear to be generated, although a small undetectable breather may be present. This is consistent with weakly nonlinear theory which predicts a longer-wave envelope as the amplitude decreases. In both of these simulations the initial perturbation may have been too narrow for the amplitude of the perturbation. For $(a,L)=(0.26,5)$ longer breathers with much longer

periods of oscillation were generated. Breathers were also generated using an initial profile consisting of two smoothed rectangular boxes, similar to that used in theoretical studies of weakly nonlinear breathers [18]. Initializing the model with a density field based on a weakly nonlinear breather with multiple oscillations resulted in a smaller-amplitude breather with the same number of oscillations.

Some differences between weakly nonlinear and fully nonlinear breathers were noted. For the first case, with $p=0.0285$, a significant difference in the propagation speed was observed in a reference frame moving with the linear long-wave propagation speed, although relative to the fluid the difference was small. In both cases the oscillations in the fully nonlinear breather were not symmetric in the sense that the maximum downward displacement was not equal to the maximum upward displacement half an oscillation period later. Both of these differences imply that higher-order nonlinear effects are of some importance.

ACKNOWLEDGMENTS

This work was supported by a grant of Canadian Foundation for Climate and Atmospheric Science (K.G.L.), RFBR No. 04-05-3900 (E.P.), RFBR No. 05-05-64333 (O.P.), RFBR No. 06-05-64232 (T.T.), and RFBR No. 06-05-64087 (A.K.)

[1] D. J. Benny, J. Math. Phys. **45**, 52 (1966).
[2] M. Funakoshi, J. Phys. Soc. Jpn. **54**, 2470 (1985).
[3] K. G. Lamb and L. Yan, Oceanogr. **26**, 2712 (1996).
[4] E. Pelinovskii, O. Polukhina, and K. G. Lamb, Oceanology (Engl. Transl.) **40**, 757 (2000).
[5] R. Grimshaw, E. Pelinovsky, and O. Poloukhina, Nonlinear Processes Geophys. **9**, 221 (2002).
[6] A. Slyunyaev and E. Pelinovsky, JETP **89**, 173 (1999).
[7] A. V. Slyunyaev, JETP **92**, 529 (2001).
[8] R. Grimshaw, D. Pelinovsky, E. Pelinovsky, and A. Slunyaev, Chaos **12**, 1070 (2002).
[9] K. A. Gorshkov, L. A. Ostrovsky, I. A. Soustova, and V. G. Irisov, Phys. Rev. E **69**, 016614 (2004).
[10] Y. Z. Miropol'sky, *Dynamics of Internal Gravity Waves in the Ocean* (Kluwer Academic, Dordrecht, 2001).
[11] K. R. Helfrich and W. K. Melville, Annu. Rev. Fluid Mech. **38**, 395 (2006).
[12] R. Grimshaw, E. Pelinovsky, and T. Talipova, Nonlinear Processes Geophys. **4**, 237 (1997).
[13] T. Talipova, E. Pelinovsky, K. Lamb, R. Grimshaw, and P. Holloway, Dokla. Earth Sci. **365**, 241 (1999).
[14] D. Pelinovsky and R. Grimshaw, Phys. Lett. A **229**, 165 (1997).
[15] K. W. Chow, R. H. J. Grimshaw, and E. Ding, Wave Motion **43**, 158 (2005).
[16] J. L. Lamb, *Elements of Soliton Theory* (John Wiley & Sons, New York, 1980).
[17] H. Takahashi and K. Konno, J. Phys. Soc. Jpn. **58**, 3085 (1989).
[18] S. Clarke, R. Grimshaw, P. Miller, E. Pelinovsky, and T. Talipova, Chaos **10**, 383 (2000).
[19] K. G. Lamb, J. Fluid Mech. **451**, 109 (2002).